Measuring cloud point pressures by image analysis: A simple and reproducible alternative method to direct visual determination

Mingxi Wang, Simon Harrisson, Mathias Destarac, Jean-Daniel Marty

Contents lists available at ScienceDirect

The Journal of Supercritical Fluids

journal homepage: www.elsevier.com/locate/supflu

Measuring cloud point pressures by image analysis: a simple and reproducible alternative method to direct visual determination

Mingxi Wang,[a] Simon Harrisson,[a] Mathias Destarac,[a,*] Jean-Daniel Marty[a,*]

[a] IMRCP, UMR 5623, Université de Toulouse, 118, route de Narbonne, F-31062 Toulouse, Cedex 9, France

GRAPHICAL ABSTRACT

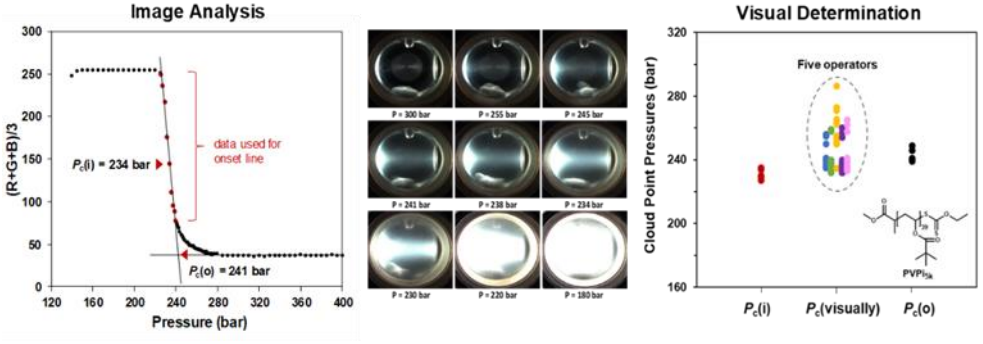

ARTICLE INFO

Keywords:
Solubility
Cloud point
Block copolymer
Supercritical carbon dioxide

ABSTRACT

In this work, we propose an easy to implement and use methodology to measure cloud point pressures in supercritical carbon dioxide without the need for a specific setup. This method is based on the analysis of images issued from the video recording of solution changes occurring while the pressure is changed. This alternative analytical method demonstrates higher repeatability, higher accuracy than direct visual determination and enables in the case of complex architectures like block copolymers to infer additional information from cloud point measurements.

1. Introduction

Supercritical carbon dioxide ($scCO_2$) has emerged as a major research field over the past twenty years. Many works focused on its potential as a reaction medium for organic chemistry and polymer synthesis.[1-6] From this, $scCO_2$ appeared a poor solvent because of its non-polar nature and its low cohesive energy density. In the field of polymer science, the identification of CO_2-soluble polymers and rationalization of their solubility properties have thus represented major challenges either to stabilize nanostructures in $scCO_2$ (emulsions, microemulsions…)[7] or to control the morphology of nanomaterials obtained from them.[1, 5, 8-10] Enthalpic and entropic effects have to be taken into account when considering the solubility of polymeric species.[11] To favor solubility, enthalpic solvent/compound interactions have to be larger than solvent/solvent or compound/compound interactions. Nevertheless, as in the case of conventional solvents, enthalpic effects cannot solely explain the difference of solubility observed in supercritical fluids, especially in the case of polymers with high average molecular weight.[11] In this case, entropic effects are also involved. Many studies have been conducted to rationalize the solubility properties of the main classes of polymers in different supercritical fluids including $scCO_2$.[11]

The understanding of structure/solubility relationship requires access to theoretical and experimental methods for the estimation or determination of the solubility for given experimental conditions of pressure and temperature as well as cloud point pressure (P_c) and temperature (T_c). Various experimental methods have thus been developed to measure the solubility of chemical compounds in supercritical environments. These methods are divided into analytical and synthetic ones.

In the analytical methods, at the desired conditions of P and T the mixture separates into two or more phases and their composition is analysed either directly or by sampling under ambient pressure. Absorption techniques are typical analytical techniques used in $scCO_2$. Among them infrared spectroscopy relies on the identification of characteristic bands associated with functional groups of the solute.

* Corresponding author.
E-mail address: destarac@chimie.ups-tlse.fr; marty@chimie.ups-tlse.fr

Measuring the intensity of these bands allows to determine the concentration of the solute according to the Beer-Lambert law ($A = \varepsilon \cdot l \cdot c$ with A, sample absorbance without dimension; ε, molar extinction coefficient; l, optical path length and c, sample concentration). For instance, high-pressure infrared spectroscopy can be used to determine the solubility of polymers in $scCO_2$ by measuring the growth of a characteristic vibrational band with increasing pressure or temperature in an isochoric cell. Using the CO_2 state equation, the solubility of the polymer can be plotted as a function of CO_2 density.[12] Consequently, based on this principle many authors have reported the solubility of various polymers with different structural parameters and architectures.[13-17] This method therefore allows a quantitative determination of the solubility of a compound. However, its use remains limited because it requires the use of a highly specialized equipment and is limited to the characterization of compounds with specific chemical functionalities.

In the synthetic method the mixture is prepared inside the vessel and so the overall mixture composition is known. The appearance of phase boundaries is detected through visual examination using a view cell. Hence, most measurements of polymer solubility in scCO2 rely on repeated visual observations of phase separation transitions in a variable-volume view cell. The cell is loaded with a defined amount of polymer and a known amount of $scCO_2$. It is equipped with a sapphire window to observe the turbidity of the solution. The solution is then heated at a chosen temperature and pressurized under stirring to obtain a single phase. Then the pressure is slowly decreased until the solution becomes cloudy. The cloud point is then determined when the stirrer or the background of the cell is no longer distinguishable. This allows the determination of cloud point coordinates (P_c, T_c) for a sample at a single polymer/CO_2 ratio over a large range of temperatures. From a practical point of view, it is much more efficient to hold the system temperature constant and vary the pressure since the thermal mass of the cell is very large. The main advantage of this cloud point method is that it does not require tedious analysis to obtain solubility behavior. Nevertheless, unlike spectroscopic methods, the solubility measurement is indirect and can be distorted by several factors: first, the presence of impurities can induce nucleation of polymer provoke cloudiness during the cloud-point pressure determination at pressures higher than the ones observed for pure polymer. Moreover, this method is based on the formation of aggregates in solution induced by a change in the density of the supercritical medium (due to a change in pressure or temperature). Visual determination of transition parameters is therefore only possible when aggregates of sufficient size are present in solution and thus scatter light. Hence, even for pure polymer, the kinetics of formation of aggregates, the concentration of the compound and the rate of depressurization or cooling, the subjective choice of the transition zone are thus parameters that can limit the precision of the measurement of the transition parameters P_c and T_c through this visual method. The accuracy of the measurements can be significantly improved by coupling the cells with scattering measurements (light,[18] neutron,[19, 20] X-ray [21]) allowing earlier measurement of the formed aggregates. Nevertheless as for spectroscopic methods the implementation of these coupled methods is much more complex and remains relatively uncommon in the literature.

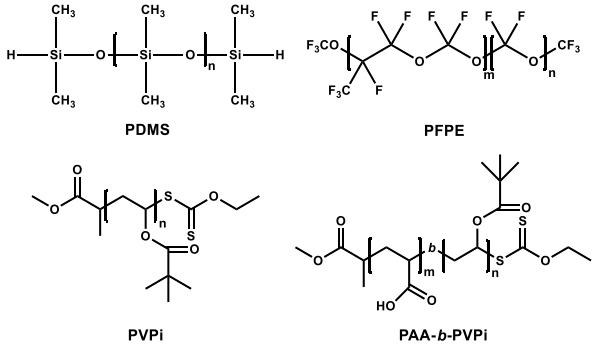

Scheme 1. The chemical structure of the different polymers used.

There is therefore a particular interest in optimizing the measurement of transitions based on direct observation. For instance, some setup enable to register the change in the transmitted light intensity through the cell but still require a two-window experimental setup or a fiber optic light source and detector. The phase separation pressure for a chosen temperature is then evaluated from the transmitted intensity as the pressure corresponding to the onset of the deviation from the baseline transmitted light intensity or to a chosen level of transmitted light.[22, 23] Nowadays these measurements are most often combined with video recording. In this article we first propose to validate and evaluate an approach based on the further processing of the images obtained from these recordings. For this an average value of red, blue and green component of an area of the recording is followed as a function of CO_2 pressure. The validity of solubility measurements through this method is first studied through the analysis and solubility of different types of polymers, namely polydimethylsiloxane (PDMS), perfluoropolyether (PFPE) and poly(vinyl pivalate) (PVPi). (Scheme 1). The accuracy and precision (repeatability and reproducibility) is compared to a direct visual determination. Additionally, the influence of depressurization rates and polymer concentration on the measurement is evaluated. In a second step, we demonstrate the interest of this method for the study of transition phenomena involving more structurally complex poly(acrylic acid)-poly(vinyl pivalate) block polymers.

2. Experimental section

2.1. Materials

Acrylic acid (AA, Aldrich, 99%), vinyl pivalate (VPi, Aldrich, 98%), polydimethylsiloxane (PDMS, hydride terminated, viscosity 100 cSt, M_w = 6000 g mol^{-1}, Abcr GmbH), perfluoropolyether (PFPE, Fomblin® Y, LVAC 25/6, viscosity 270 cSt, M_w = 3300 g mol^{-1}, Sigma Aldrich), trimethylsilyldiazomethane (2M solution in diethyl ether, Acros Organics), tetrahydrofuran (THF for preparative HPLC, stabilized with BHT, SDS) and carbon dioxide (CO_2 N45 TP, Air Liquide) were used as received. Ethyl acetate (Fischer Scientific, Laboratory reagent grade) and 1,4-dioxane (Aldrich, 98%) were distilled on CaH_2. 2,2-Azobisisobutyronitrile (AIBN, Acros Organics, 98%) was recrystallized twice from methanol and dried under vacuum. Xanthate X1 has been synthesized according to an earlier procedure from our group.[24] The homopolymer $PVPi_{5k}$ and the block copolymers PAA-*b*-PVPi were synthesized by reversible addition–fragmentation chain transfer/macromolecular design via the interchange of xanthates (RAFT/MADIX) polymerization with Xanthate X1 as the chain transfer agent (see supporting information).

2.2. Determination of the solubility in $scCO_2$

Solubility measurements of the polymer in $scCO_2$were obtained using a high-pressure phase equilibrium apparatus (Top Industrie, France) to measure cloud points. This high-pressure unit is composed of a variable volume view cell (from 9.6 to 31.3 cm^3 by using a piston) equipped with two sapphire windows and a magnetic stirrer. The temperature of the cell was maintained at 40 °C by a thermostated bath. Temperature was measured by a thermocouple (J type, precision of ± 0.1 K) placed in the center of the cell. Pressure was measured using a pressure transducer (Keller) equipped with a pressure numerical display. The change of solution turbidity was filmed with a camera and observed on a video screen (see Figure S1).

In a typical experiment, 40 mg (0.2 wt.%) of the polymer sample was weighed and transferred into the main chamber of the cell with the stirring bar. The cell was sealed and CO_2 (20.0 g) thermostated at 2 °C was injected into the cell by an automatic syringe pump (260D, Teledyne ISCO). The cell was then heated to 40 °C and was pressurized at 400 bar by decreasing the volume of the cell. The polymer was observed to completely dissolve in $scCO_2$ and the homogeneous polymer-CO_2 solution appeared. A video was started and the system pressure during the whole procedure was recorded from this time. After the system was equilibrated under stirring for 10 min, the pressure inside the cell was slowly reduced at different depressurization rates (i.e. 2, 5, 10, 15 and 20 bar/min) until the maximum volume was restored. The grey intensity of some images captured from the obtained video was calculated from red (R), green (G) and blue (B) component of the image as (R+G+B)/3 values thanks to the software ImageJ (Figure S2).

For reproducibility measurements performed on $PVPi_{5k}$ at 0.2 wt.%, five different samples were prepared independently. Cloud point pressures were obtained either by analyzing grey intensity: P_c(o) and P_c(i) of these five samples or by direct visual determination from video recording by five different operators: P_c(visually) (each one of the five samples is evaluated three times in a blind experiment by each operator). Analysis of collected

results was performed using the recommendations of standard ISO 5725 and 17025 or by gage repeatability and reproducibility analysis.

3. Results and discussion

3.1. Methodology of measurements.

The solubility of the polymers was measured using a variable volume view cell (Figure S1 and S2 in supporting information). The temperature of the cell was maintained at 40 °C and the pressure inside the cell was slowly reduced at different depressurization rates (i.e. 2, 5, 10, 15 and 20 bar·min^{-1}). Phase changes occurring in the cell are filmed with a camera. This recording is then used to extract the greyscale intensity of a selected area from the measured RGB color codes (i.e. (R+G+B)/3) using the ImageJ software. This value is reported as a function of the measured pressure. Figure 1 illustrates this method for a PVPi homopolymer (PVPi$_{5k}$, M_n = 4980 g·mol^{-1}, Đ = 1.12, see supporting information for polymer synthesis and characterization). Figure 1A shows typical photos registered at different pressures. Analysis of grey intensity enables to obtain the curve presented in Figure 1B. The cloud point pressures are then evaluated from the curve obtained either by estimating the onset value (P_c(o)) or by measuring its inflection point (P_c(i)). In the case of PVPi these two values are respectively equal to 241 and 234 bar. Visually, the cloud point pressure was estimated at 240 bar, i.e. between the two previous values and near the inflexion point P_c(i). The visual determination is indeed hampered by the difficulty to precisely define the transition point and requires reaching a sufficient level of scattering to be determined. This visual value is therefore highly dependent on the assessment of the experimenter (*vide infra*).

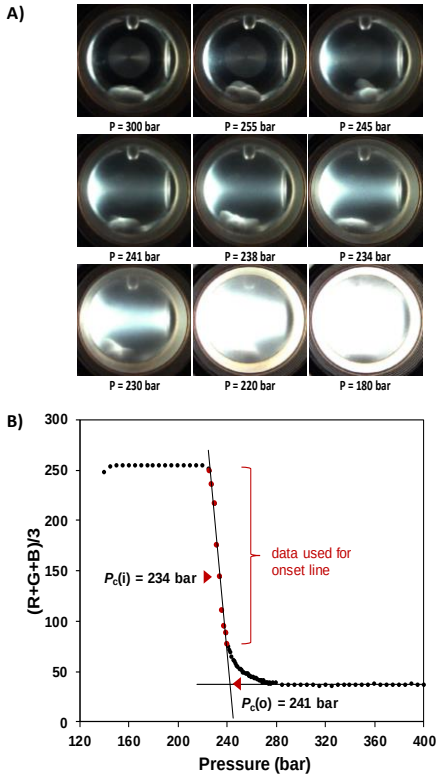

Figure 1. A) Photos of a typical cloud point measurement; and B) variation of (R+G+B)/3 with pressure and the way to define cloud point pressures P_c(o) and P_c(i), under a depressurization rate of 10 bar/min at 40 °C for PVPi$_{5k}$ (0.2 wt.%) in scCO$_2$.

The validation of this numerical approach to determine cloud point pressures was carried out following the recommendations of standard ISO 5725 and 17025. The reproducibility of the method is estimated from a series of five independent measurements (see Figure S3 in supporting information). From this, the coefficient of variation (CV) of reproducibility, i.e. the ratio of the standard deviation to the mean, is calculated to give a measure of the dispersion of data points around the mean. This value is then compared to the one issued from visual determination (in a blind experiment each operator evaluates P_c(visually) three times) for each one of the five samples prepared, see Figure 2). CV of reproducibility values equal to 1.6% and 4.2% are found for computational and visual methods respectively. The newly proposed method here offers significantly improved reproducibility compared to the direct visualization method. Gage repeatability and reproducibility analysis performed on the visual method confirmed that the main parameter responsible for measurement variability is the operator (40 % of total variation) and the preparation of sample (55 % of total variation). Hence, the improvement in fidelity previously mentioned is mainly due to the minimization of the experimental error linked to the often difficult assessment of the cloud point pressure by the operator which is replaced by a numerical approach in the proposed method. The cloud point pressure can thus be determined in a more accurate way through the analysis of videos.

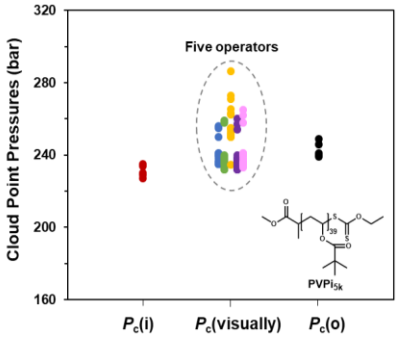

Figure 2. Illustration of reproducibility issues for the measurement of cloud point pressures of PVPi$_{5k}$ samples (0.2 wt.%) either by analyzing grey intensity: P_c(o) and P_c(i) or by direct visual determination from video recording by five different operators: P_c(visually) (a given sample is evaluated three times in a blind experiment by each operator).

3.2. Effect of concentration and rate of depressurization on the fidelity of cloud point measurements.

Among the main parameters which influenced the results, some of them are related to experimental conditions, e.g. rate of depressurization or polymer concentration.[23] In order to further compare the proposed method to the visual one, we first compare the effect of rate of depressurization on the cloud point measurement in the case of PVPi$_{5k}$ as illustrated in Figure 3.

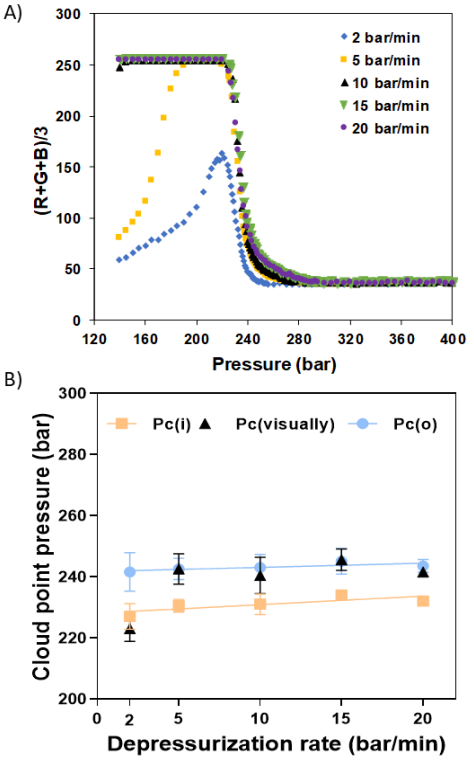

Figure 3. A) Variation of (R+G+B)/3 with pressure under different depressurization rates (◆2 bar/min, ■5 bar/min, ▲10 bar/min, ▼15 bar/min and ●20 bar/min); and B) variation of cloud point pressures (■P_c(i) ▲P_c(visually) and ●P_c(o)) with different depressurization rates; at 40 °C for PVPi$_{5k}$ (0.2 wt.%) in scCO$_2$.

The profiles of grey intensity variation as a function of pressure (Figure 3A) are strongly influenced by this rate. Especially at low speeds the maximum intensity values obtained are lower. These differences are in particular related to solution aggregation processes of different polymer chains. High depressurization rate favor the formation of highly diffusing aggregates. The assessment of cloud point pressures, P_c(o) and P_c(i), from these curves is shown in Figure 3B and compared with P_c(visually). When the depressurization rate decreased from 20 to 2 bar/min, the direct visual determination of cloud point pressure showed a slight decrease of P_c(visually) from 252 to 226 bar, i.e. a 10% change. At a 5% risk level, this effect is found to be significant (p value < 0.05). Nevertheless, such an effect is no more significant when cloud point pressures P_c(o) and P_c(i) were determined by image analysis from Figure 3A. Such a difference might arise from the reproducibility issues (see section 3.1) and from the aforementioned lower scattering level observed at lower depressurization rate that renders the visual determination less accurate. A depressurization rate of 10 bar/min was chosen in the following experiments.

The effect of concentration on the fidelity and accuracy of measurements is then determined in the range 0.02 wt.% to 1 wt.% (Figure 4). As expected, the concentration of polymer in solution has a strong influence on the value of cloud point pressure (Figure 4B) : while at a concentration of 1 wt.% the cloud point pressure P_c(i) is estimated at 269 bar, this measurement at a concentration of 0.02 wt.% leads to a value of P_c(i) equal to 165 bar. This dependence on concentration is mainly related to thermodynamic solubilization effect and is expected for such a range of concentration.[23] Moreover, determination of cloud point pressures led to P_c(o) > P_c(visually) > P_c(i) whatever the concentration used. The main differences between visual determination and image analysis arise from the higher repeatability of the latter at lower concentration. Indeed while standard deviation of repeatability related to visual determination is equal to 0.7 bar at 0.2 wt.% (for a standard deviation of reproducibility equal to 13 bar, see previous results), this standard deviation of repeatability increased up to 2.8 bar at 0.02 wt.%. Figure 4A shows that, at the chosen depressurization rate (10 bar/min), all the solutions became highly diffusive once the transition is reached. Nevertheless, a lower maximum grey intensity was measured for the solution with the lowest concentrations (i.e. 0.02 and 0.05 wt.%). This phenomenon, related to lower diffusing properties due to the decreasing number of diffusing centers observed, hampered the precise determination of cloud point pressure visually. At the same time, standard deviation issued from analysis of grey intensity remains roughly constant (standard deviation of reproducibility equal to 3 bar) as this determination does not require high level of scattering to be performed.

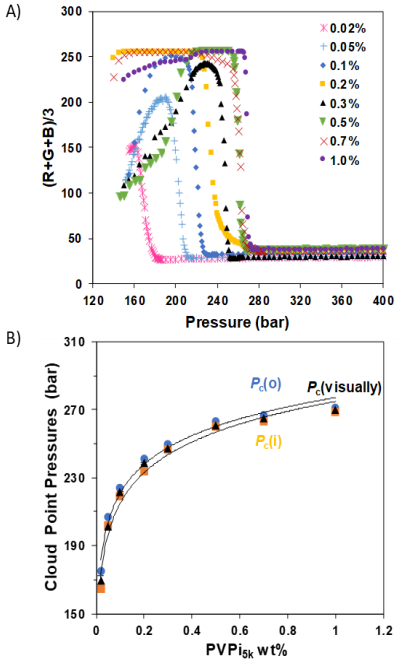

Figure 4. A) Variation of (R+G+B)/3 with pressure for eight different polymer concentrations (wt.%) under a depressurization rate of 10 bar/min at 40 °C for $PVPi_{5k}$ in $scCO_2$; and B) variation of cloud point pressures (■P_c(i) ▲P_c(visually) and ●P_c(o)) with different concentrations of polymer; at 40 °C for $PVPi_{5k}$ in $scCO_2$.

Therefore, the determination of cloud point pressure by using the analysis of grey intensity enables to enlarge the choice of experimental parameters (rate of depressurization and concentration) while having a satisfactory reproducibility of measurements compared to direct visual determination. Indeed for the latter, obtaining a reproducible and accurate measurement requires the use of a sufficient concentration (above 0.1 wt.% for $PVPi_{5k}$) and depressurization rate fast enough to favor the formation of large enough aggregates to diffuse light at a sufficient level.

3.3. Evaluation of the methodology on different types of polymers.

Additionally to these experimental parameters, structural parameters such as the polymer architecture, molecular weight and nature of end groups significantly affected the results. A polymer with a high molecular weight will favor the formation of larger aggregates at lower concentration. This parameter will not be considered here. Chemical parameters will also play a role on the aggregation process occurring during the measurement of cloud point pressure. Fluoropolymers, [25, 26] polysiloxanes [27-29] and, to a lesser extent, poly(vinyl esters) [30-33] are regarded as standard CO_2-philic polymers with well described solubility properties. A representative of each family, i.e. PFPE (Fomblin® Y, M_w = 3300 g·mol^{-1}), PDMS (M_w = 6000 g·mol^{-1}) and PVPi ($PVPi_{5k}$, M_n = 4980 g·mol^{-1}) was studied as described in the first part of this paper (see Figure S4-S7 in supporting information). Figure 5 shows the variation of grey intensity with pressure under a depressurization rate of 10 bar/min at 40 °C for these three polymers.

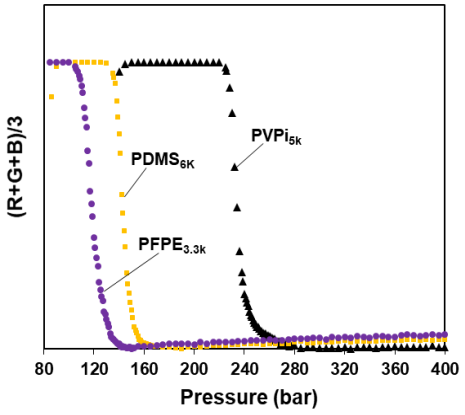

Figure 5. Variation of (R+G+B)/3 with pressure under a depressurization rate of 10 bar/min at 40 °C for different polymers (▲$PVPi_{5k}$, ■$PDMS_{6k}$ and ●$PFPE_{3.3k}$, 0.2 wt.%) in $scCO_2$.

The cloud point pressures are then evaluated from these curves. In the case of PDMS, P_c(i) and P_c(o) are respectively equal to 141 ± 0.5 and 146 ± 1.5 bar. Visually, the cloud point pressure was estimated at 147 ± 4.5 bar. Values near P_c(o) were found visually for PDMS for which a rapid and strongly pronounced slope breaking of the curve is observed. For PFPE, P_c(i) and P_c(o) are respectively equal to 115 ± 1.3 bar and 122 ± 0.9 bar. Visually, the cloud point pressure was estimated at 120 ± 2.5 bar. In the case of $PVPi_{5k}$ the initial change of scattered intensity is slower; therefore visual determination of P_c(visually) was found near P_c(i). The reproducibility of measurements was evaluated for all three polymers and CV of reproducibility for P_c(o) was found equal to 0.8%, 1.0% and 1.8% for PFPE, PDMS and PVPi respectively. These values are significantly better than the ones obtained visually (2.3%, 1.9% and 5.7% respectively). In the case of PDMS and PFPE, no significant influence of depressurization rate on cloud point pressure was determined (either visually or from the analysis of grey intensity).

The solubility behavior of polymers with more complex structures (statistical, block, graft, star, hyperbranched…) is the subject of numerous studies as they have demonstrated to be of great interest to stabilize water/CO_2 interfaces. Nevertheless, their complex structures may render the determination of cloud point pressure a more complicated task. We illustrate this by studying two block copolymers based on $PVPi_{5k}$ and poly(acrylic acid) (PAA): PAA_{1k}-*b*-$PVPi_{4k}$ and $PAA_{0.5k}$-*b*-$PVPi_{4.5k}$ (Scheme 1, Figure S8-S10 in supporting information).

As can be seen in Figure 6A, at a given depressurization rate, the variation

of grey intensity shows a change of slope which significantly complicates the determination of the cloud point pressure. Thus at a depressurization rate of 10 bar/min, P_c(i) and P_c(o) are respectively equal to 258 and 293 bar. Visually, the cloud point pressure was estimated at 289 bar. Moreover, the profiles of the curves depend strongly on the depressurization rate: low diffusiveness of the observed solutions was obtained at low depressurization rates. This phenomenon is much more pronounced than in the case of homopolymers. These observations can be related as mentioned above to kinetic phenomena related to the aggregation process. In addition, these block structures are likely to form colloidal structures of nanometric size (and therefore poorly-diffusing). Interestingly, contrary to what was observed for homopolymers, a significant decrease of P_c(o), P_c(i) and P_c(visually) was observed when the rate of depressurization decreased. Nevertheless the measured effect is less pronounced in the case of grey intensity approach. A more precise value of cloud point pressure, close to the one obtained at equilibrium, can be easily obtained from Figure 6B by extrapolating the line at a depressurization rate of 0°C/min. The coefficient of variation of reproducibility for P_c(o) and P_c(i) were found equal to 1.3% and 1.7% respectively at a depressurization rate of 10 bar/min. These values are significantly better than the one obtained visually, i.e. 3.4%. The same behavior is observed for the second studied copolymer PAA_{1k}-*b*-$PVPi_{5k}$.

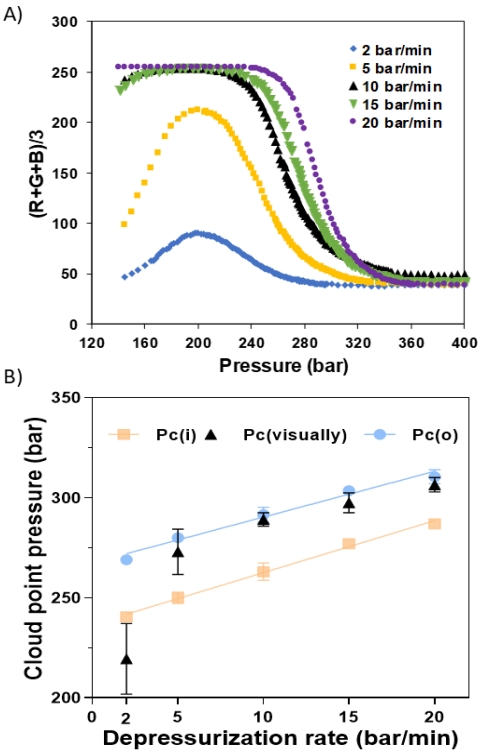

Figure 6. A) Variation of (R+G+B)/3 with pressure under different depressurization rates (♦2 bar/min, ■5 bar/min, ▲10 bar/min, ▼15 bar/min and ●20 bar/min); and B) variation of cloud point pressures (■P_c(i) ▲P_c(visually) and ●P_c(o)) with different depressurization rates; at 40 °C for $PAA_{0.5k}$-*b*-$PVPi_{4.5k}$ (0.2 wt.%) in $scCO_2$.

Figure 7 summarizes all the results obtained for the cloud point pressures P_c(o), P_c(i) and P_c(visually) of the different types of polymers studied in this article (with associated standard deviation). From this it can be concluded that the approach proposed here enables to significantly increase the fidelity of measurements compared to the usual visual determination whatever the polymer is (figure S11 in supporting information). Of special interest is the case of polymer with more complex structures (here block copolymers) for which this method enables to obtain more reproducible results and get information on the process of aggregation occurring in solution.

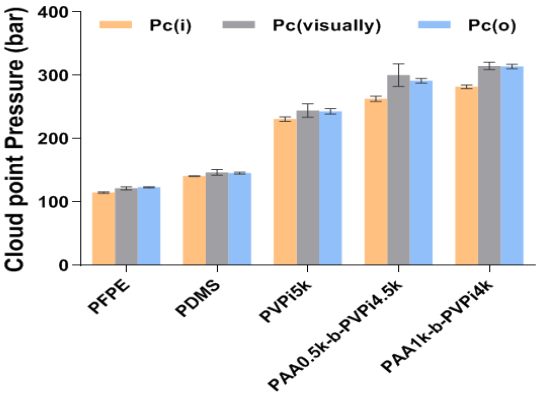

Figure 7. Cloud point pressure for different polymers determined either visually (P_c(visually) or by analyzing images (P_c(i) and P_c(o)) with corresponding standard deviation errors (depressurization rate equal to 10 bar/min).

4. Conclusion

In this work, we propose an easy to implement and use methodology to measure cloud point pressures for polymers of different chemical nature and architecture. This method is based on the analysis of images of solution-phase changes with changes in pressure. Results were compared to the ones obtained by direct visual observation. This alternative method demonstrates higher reproducibility and higher accuracy than direct visualization method for which strong inter-operator variations exist. It demonstrates the importance of standardized conditions for the P_c measurement, particularly for block copolymers. By using this method, we estimate the effect of different parameters (experimental or structural) on the value of cloud point pressure. In contrast to the visual method, the proposed method is much less affected by the level of scattering of the studied solution, which confers an increased reproducibility on the measurement. Interestingly, the proposed methodology enables in the case of complex architecture like block copolymer to infer information on the mechanism of aggregation and to greatly improve the reproducibility of the measurement.

Acknowledgements

M.-X. W. would like to acknowledge the China Scholarship Council (CSC) for Ph.D. funding.

References

[1] E.J. Beckman, Supercritical and near-critical CO_2 in green chemical synthesis and processing, J. Supercrit. Fluids 28 (2004) 121-191.

[2] J.L. Kendall, D.A. Canelas, J.L. Young, J.M. DeSimone, Polymerizations in supercritical carbon dioxide, Chem. Rev. 99 (1999) 543-564.

[3] L. Du, J.Y. Kelly, G.W. Roberts, J.M. DeSimone, Fluoropolymer synthesis in supercritical carbon dioxide, J. Supercrit. Fluids 47 (2009) 447-457.

[4] B. Zetterlund, F. Aldabbagh, M. Okubo, Controlled/living heterogeneous radical polymerization in supercritical carbon dioxide, Journal of Polymer Science Part A: Polymer Chemistry 47 (2009) 3711-3728.

[5] A.I. Cooper, Polymer synthesis and processing using supercritical carbon dioxide, Journal of Materials Chemistry 10 (2000) 207-234.

[6] C. Boyère, C. Jérôme, A. Debuigne, Input of supercritical carbon dioxide to polymer synthesis: An overview, European Polymer Journal, 61 (2014) 45-63.

[7] D.L. Tomasko, H. Li, D. Liu, X. Han, M. J. Wingert, L. J. Lee, K.W. Koelling, A review of CO_2 applications in the processing of polymers, Ind. Eng. Chem. Res. 42 (2003) 6431-6456.

[8] H.M. Woods, M.M. Silva, C. Nouvel, K.M. Shakesheff, S.M. Howdle, Materials processing in supercritical carbon dioxide: surfactants, polymers and biomaterials, J. Mater. Chem. 14 (2004) 1663-1678.

[9] F. Cansell, C. Aymonier, Design of functional nanostructured materials using supercritical fluids, J. Supercrit. Fluids 47 (2009) 508-516.
[10] C. Aymonier, A. Loppinet-Serani, H. Reverón, Y. Garrabos, F. Cansell, Review of supercritical fluids in inorganic materials science, J. Supercrit. Fluids 38 (2006) 242-251.
[11] E. Girard, T. Tassaing, J.-D. Marty, M. Destarac, Structure–property relationships in CO_2-philic (co)polymers: phase behavior, self-assembly, and stabilization of water/CO_2 emulsions, Chem. Rev. 116 (2016) 4125-4169.
[12] S.K. Kumar, K.P. Johnston, Modelling the solubility of solids in supercritical fluids with density as the independent variable, J. Supercrit. Fluids 1 (1988) 15-22.
[13] V. Martinez, S. Mecking, T. Tassaing, M. Besnard, S. Moisan, F. Cansell, C. Aymonier, Dendritic Core−shell macromolecules soluble in supercritical carbon dioxide, Macromolecules 39 (2006) 3978-3979.
[14] Y. Danten, T. Tassaing, M. Besnard, Vibrational spectra of CO_2-electron donor−acceptor complexes from ab initio, J. Phys. Chem. A 106 (2002) 11831-11840.
[15] E. Girard, T. Tassaing, J.-D. Marty, M. Destarac, Influence of macromolecular characteristics of RAFT/MADIX poly (vinyl acetate)-based (co) polymers on their solubility in supercritical carbon dioxide, Polym. Chem. 2 (2011) 2222-2230.
[16] A. Boyer, E. Cloutet, T. Tassaing, B. Gadenne, C. Alfos, H. Cramail, Solubility in CO_2 and carbonation studies of epoxidized fatty acid diesters: towards novel precursors for polyurethane synthesis, Green chemistry 12 (2010) 2205-2213.
[17] J.-G. Chen, X. Liu, Z.-W. Liu, D.-D. Hu, C. Zhang, D. Xue, J. Xiao, Z.-T. Liu, Intermolecular-interaction-dominated solvation behaviors of liquid monomers and polymers in gaseous and supercritical carbon dioxide, Macromolecules 45 (2012) 4907-4919.
[18] S. Zhou, B. Chu, Laser light scattering study of pressure-induced micellization of a diblock copolymer of poly (1, 1-dihydroperfluorooctylacrylate) and poly (vinyl acetate) in supercritical carbon dioxide, Macromolecules 31 (1998) 5300-5308.
[19] D. Chillura-Martino, R. Triolo, J.B. McClain, J.R. Combes, D.B. Betts, D.A. Canelas, J.M. DeSimone, E.T. Samulski, H.D. Cochran, J.D. Londono, G.D. Wignallc, Neutron scattering characterization of homopolymers and graft-copolymer micelles in supercritical carbon dioxide, Journal of Molecular Structure 383 (1996) 3-10.
[20] G.D. Wignall, Neutron scattering studies of polymers in supercritical carbon dioxide, Journal of Physics: Condensed Matter 11 (1999) R157-R177.
[21] J.L. Fulton, D.M. Pfund, J.B. McClain, T.J. Romack, E.E. Maury, J.R. Combes, E.T. Samulski, J.M. DeSimone, M. Capel, Aggregation of amphiphilic molecules in supercritical carbon dioxide: a small angle X-ray scattering study, Langmuir 11 (1995) 4241-4249.
[22] K. Liu, E. Kiran, Miscibility, viscosity and density of poly (ε-caprolactone) in acetone + CO_2 binary fluid mixtures, J. Supercrit. Fluids 39 (2006) 192-200.
[23] C. F. Kirby, M.A. McHugh, Phase behavior of polymers in supercritical fluid solvents, Chem. Rev. 99 (1999) 565-602.
[24] X. Liu, O. Coutelier, S. Harrisson, T. Tassaing, J.-D. Marty, M. Destarac, Enhanced solubility of polyvinyl esters in $scCO_2$ by means of vinyl trifluorobutyrate monomer, ACS Macro Lett. 4 (2015) 89-93.
[25] F.E. Henon, M. Camaiti, A.L.C. Burke, R.G. Carbonell, J.M. DeSimone, F. Piacenti, Supercritical CO_2 as a solvent for polymeric stone protective materials, J. Supercrit. Fluids 15 (1999) 173-179.
[26] D.A. Newman, T.A. Hoefling, R.R. Beitle, E.J. Beckman, R.M. Enick, Phase behavior of fluoroether-functional amphiphiles in supercritical carbon dioxide, J. Supercrit. Fluids 6 (1993) 205-210.
[27] Y. Xiong, E. Kiran, Miscibility, density and viscosity of poly (dimethylsiloxane) in supercritical carbon dioxide, Polymer 36 (1995) 4817-4826.
[28] Z. Bayraktar, E. Kiran, Miscibility, phase separation, and volumetric properties in solutions of poly (dimethylsiloxane) in supercritical carbon dioxide, Journal of applied polymer science 75 (2000) 1397-1403.
[29] J.J. Lee, S.D. Cummings, E.J. Beckman, R.M. Enick, W.A. Burgess, M.D. Doherty, M.J. O'Brien, R.J. Perry, The solubility of low molecular weight poly (dimethyl siloxane) in dense CO_2 and its use as a CO_2-philic segment, J. Supercrit. Fluids 119 (2017) 17-25.
[30] S. Zhang, K. Chen, L. Liang, B. Tan, Synthesis of oligomer vinyl acetate with different topologies by RAFT/MADIX method and their phase behaviour in supercritical carbon dioxide, Polymer 54 (2013) 5303-5309.
[31] D.D. Hu, Y. Zhang, M. Su, L. Bao, L. Zhao, T. Liu, Effect of molecular weight on CO_2-philicity of poly (vinyl acetate) with different molecular chain structure, J. Supercrit. Fluids 118 (2016) 96-106.
[32] N.A. Birkin, N.J. Arrowsmith, E.J. Park, A.P. Richez, S.M. Howdle, Synthesis and application of new CO_2-soluble vinyl pivalate hydrocarbon stabilisers *via* RAFT polymerisation, Polym. Chem. 2 (2011) 1293-1299.
[33] N.A. Birkin, O.J. Wildig, S.M. Howdle, Effects of poly (vinyl pivalate)-based stabiliser architecture on CO_2-solubility and stabilising ability in dispersion polymerisation of N-vinyl pyrrolidone, Polym. Chem. 4 (2013) 3791-3799.

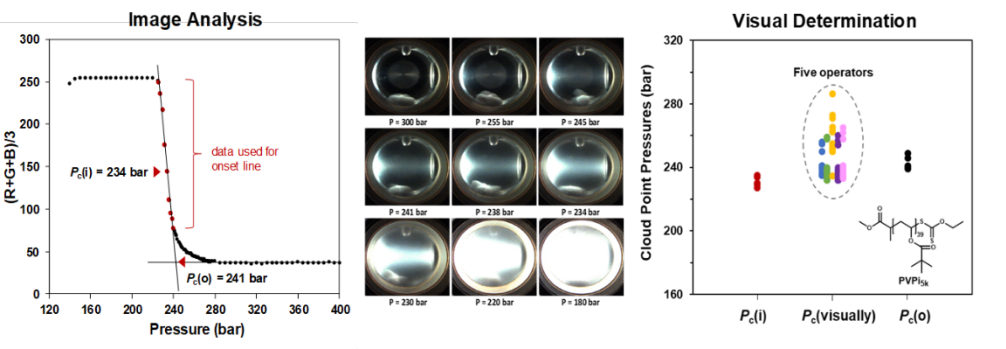
Image Analysis
(R+G+B)/3
Pressure (bar)
P_c(i) = 234 bar
P_c(o) = 241 bar
data used for onset line
P = 300 bar
P = 255 bar
P = 245 bar
P = 241 bar
P = 238 bar
P = 234 bar
P = 230 bar
P = 220 bar
P = 180 bar
Visual Determination
Cloud Point Pressures (bar)
Five operators
PVPI$_{5k}$
P_c(i)
P_c(visually)
P_c(o)